I. INTRODUCTION

In recent years, NMR/MRI portable devices [1][2] have drawn attention of numerous researcher teams. They are used for variety of applications, from medical diagnosis [3] to archaeological analysis [4], nondestructive material testing [5], evaluation of water presence in building materials [6] and food emulsions [7]. Different magnets designs have been proposed by many groups of researchers. They can be divided into two groups: the magnets *ex-situ* [8][9] and the magnets *in-situ* [10][11]. The first group has the simple configuration with the sensitive volume near their surface and the samples under test are located outside the magnets. Thus, they can be used for the experimental investigation of objects with unlimited dimensions. Although the *ex-situ* magnets have simple shape and are light weight, they are difficult to achieve in terms of homogeneity of the magnetic field in the sensitive volume.

In comparison, the *in-situ* magnets have their static field reinforced inside their bore center and canceled outside of the structure. Thus, their magnetic field is homogeneous inside the structure. The *in-situ* magnets use Halbach [11] or Aubert Configurations [17].

Starting with the proposition of Klaus Halbach in 1980 [12], the Halbach ring consists of segments of permanent magnets put together in an array. This creates a homogeneous field in the transverse plane. Based on this principle, the Halbach structure with discrete magnets for portable NMR magnet known as NMR Mandhalas was given in 2004 by Raich and Blümler [13]. It is based on an arrangement of identical bar magnets, described by the analytical equations reported in literature [14]. This concept has been widely used for building prototypes due to their easy assembly and the accessibility of their region of interest. The homogeneity of Halbach type is poor compared to traditional magnets [15]. For measurement of the relaxation times T2 and T1 or the spectrum, the inhomogeneity should not be higher than 10 ppm. To insure the sufficient field homogeneity for NMR experiments, a popular method is to add shimming magnets. The concept of movable permanent magnets in the shim unit of a Halbach array was reported by Ernesto Danieli et al [16]. Another method of shimming, based on the spherical harmonic expansion, proposes a complete procedure for permanent magnet design, fabrication, and characterization [17][18]. The advantages of Halbach structure motivated us to choose it for building our prototype.

However, increasing homogeneity while maintaining high field strength is a challenge when building NMR portable devices. In this study, we propose a light weight magnet system for NMR applications. Such system consists of two rings of 12 magnets arranged in a Halbach configuration. Its homogeneity and its magnetic field strength B0 are simulated and calculated

a, each magnet is placed at an angle $\alpha_i = i\frac{\pi}{6}$ and its magnetization is rotated by an angle $\beta_i = i\frac{\pi}{3}$. For compensation of the magnetic field outside of a ring, two others rings are placed in alignment as shown in Figure 2-b. The geometric parameters are depicted in Figure 2 and Figure 7.

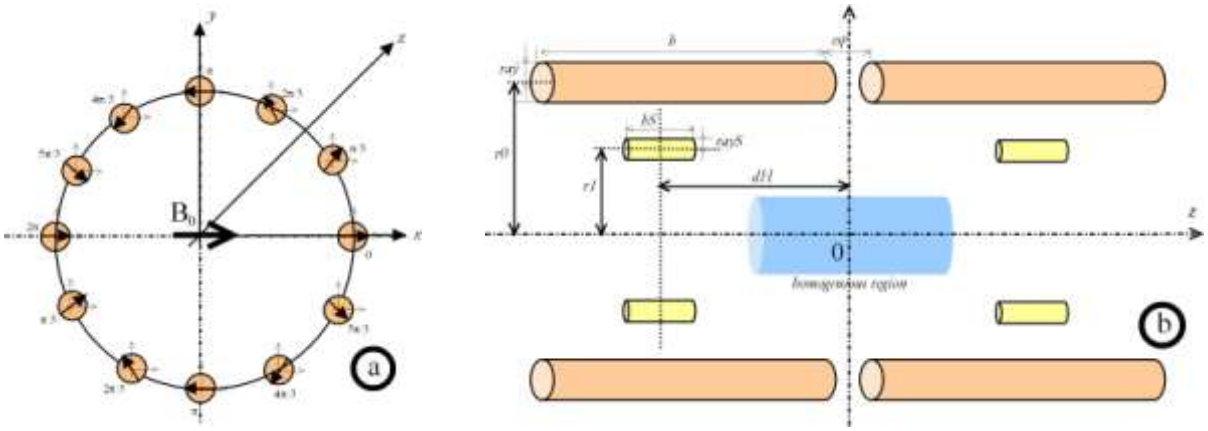

Figure 2: Position of magnets and the direction of their magnetization.

The geometric parameters are displayed in Table 1.

Table 1: Geometric parameters of our configuration.

Names of the parameter	Definitions	Dimensions
r0	Radius of the ring	30 mm
h	Height of the ring	50 mm
ray	Radius of magnets	4 mm
hS	Height of shim magnets	6 mm
rays	Radius of shim magnets	2 mm

To calculate the magnetic field of the magnet configuration, Radia [19] and Ansys [20] softwares were used. Radia was developed to design the Insertion Devices for Synchrotron light sources. It uses boundary integral methods. Each volume created to represent the magnets is subdivided in a number of sub-elements to solve the general problem of magnetization. The solution is performed by building a large matrix with represents mutual interactions between the objects.

calculated with Radia is about of 0.103 T and of 0.11 T obtained with Ansys Analysis. The difference of calculation between Radia and Ansys is about 6.79 %. This difference can be accounted for by the problem of mesh size convergence. It means that the results obtained with fine meshes are higher than those obtained with coarse meshes. Furthermore, the difference is acceptable.

Figure 3-a represents the variation of the magnetic field B0 along the Ox axis. The value of the magnetic field is almost constant for 1.8mm < x < 4.2mm. Figure 3-b represents the variation of the magnetic field B0 in the plane xOy. Each shades of color represent a variation of 50 ppm of the inhomogeneity $\frac{\Delta B_0}{B_0}$. In a rectangle of 5 × 6.4 mm^2, the inhomogeneity $\frac{\Delta B_0}{B_0}$ is larger than 450 ppm (Radia) and 380 ppm (Ansys). For an inhomogeneity lower than 100 ppm, the expected volume for experiment is 3 × 3 × 3 mm^3.

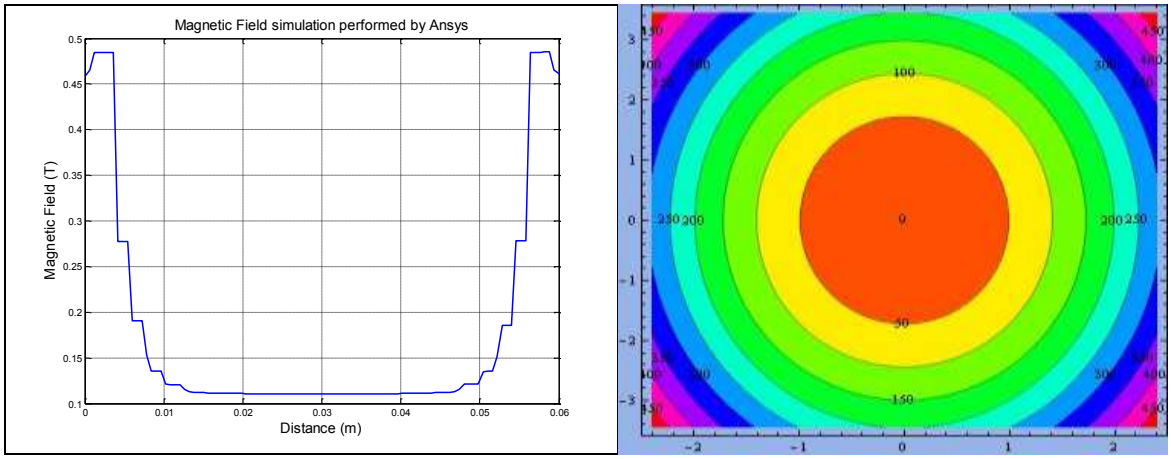

(a) Variation of magnetic field Bx versus x. (b) Inhomogeneity of the magnetic field Bx versus x and y.

Figure 3: Magnetic Field Bx distribution at z = 0 (xOy plane).

The variation of the magnetic field Bx on the xOz plane is shown in Figure 4. The magnetic field homogeneity in a region of 5 x 6.4 mm² is about 300 ppm determined by Radia, while Ansys gives a result of 200 ppm.

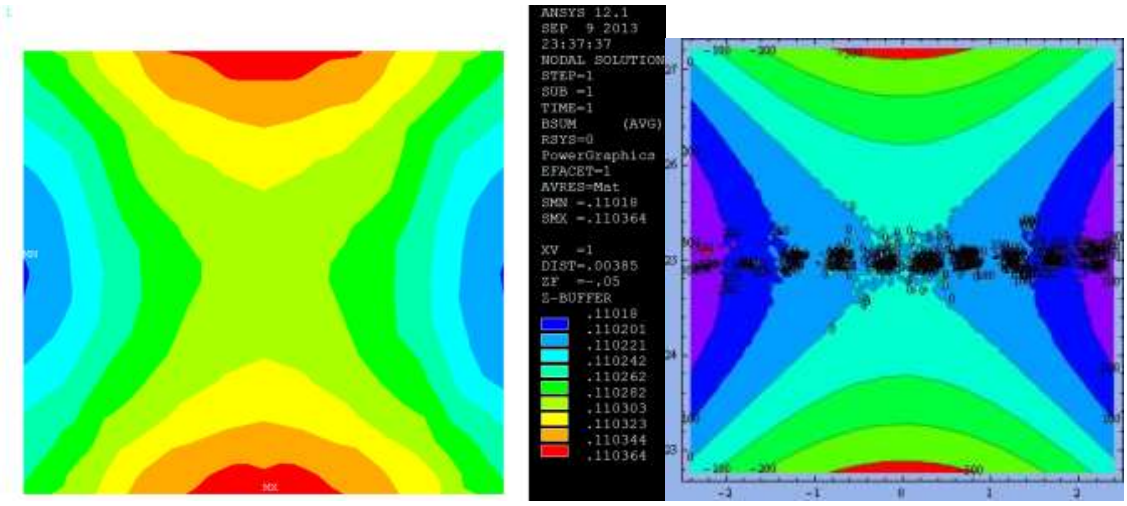

(a) Ansys Result. (b) Radia Result.

Figure 4: Magnetic Field Bx distribution in the region of 5 x 6.4 mm² in xOz plane.

The variation of profile of the magnetic field Bx along Oz axis depends on the *esp* gap between the two rings. To optimize this gap, we increased the value of *esp* by steps of 0.1mm. Figure 5 shows Bx profile for four values of *esp*. When *esp* = 0, the magnetic field outside one ring does not compensate exactly the one of the other ring. For *esp* = 0.9 mm, the compensation is optimum and the magnetic field at the center is almost constant.

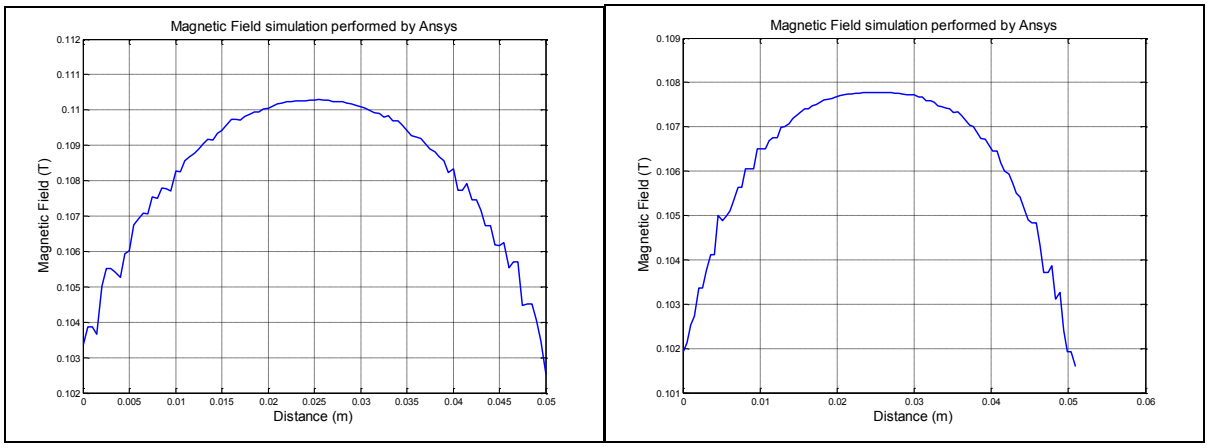

(a) *esp* = 0 mm. (b) *esp* = 0.5 mm.

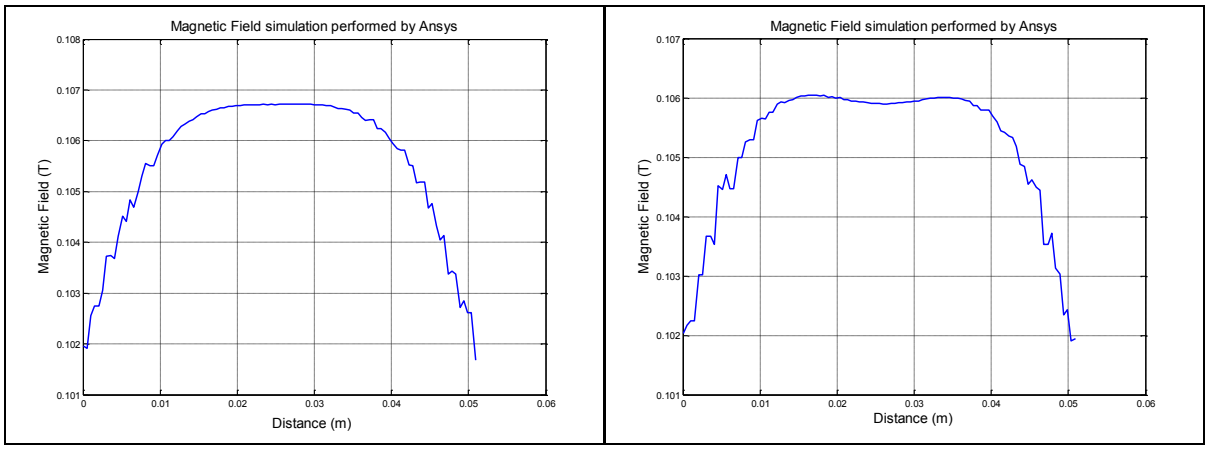

(c) *esp* = 0.9 mm. (d) *esp* = 1.3 mm.

Figure 5: The field profile for different values of the gap *esp* between the two rings.

The "useful" volume for NMR sample is determined from the coordinates (x,y,z) of the point where Bx is maximal. Then, the volume is calculated with the coordinates (x,y,z) that generate a variation of $\frac{\Delta B_0}{B_0}$ not higher than 100 ppm. The Figure 6 shows that the volume of the homogeneous region is a function of the *esp*. The optimal value of *esp* determined by Radia is around 0.77 mm and the "useful" volume is about 2640 mm^3. When the spacing *esp* between the two rings is optimized, the "useful" volume is increased by a ratio of around 80. This is caused by the decrease of the magnetic field outside one ring, which is similar to the increase of the other ring. There's an optimum gap between the two rings where the sum of the variations of the magnetic field outside the rings are canceled.

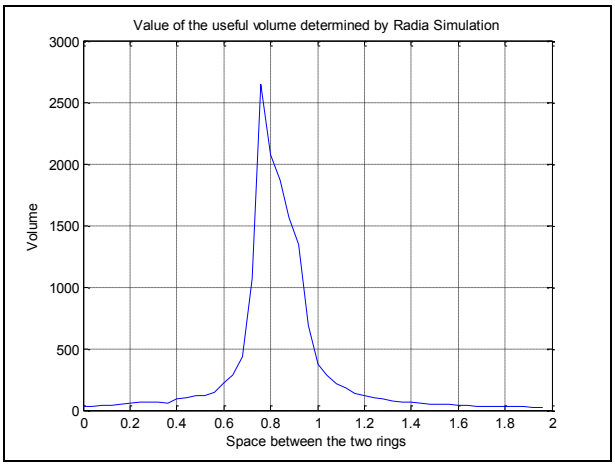

Figure 6: Volume (mm^3) for a variation of $\frac{\Delta B_0}{B_0}$ lower than 100 ppm is a function of the gap *esp*.

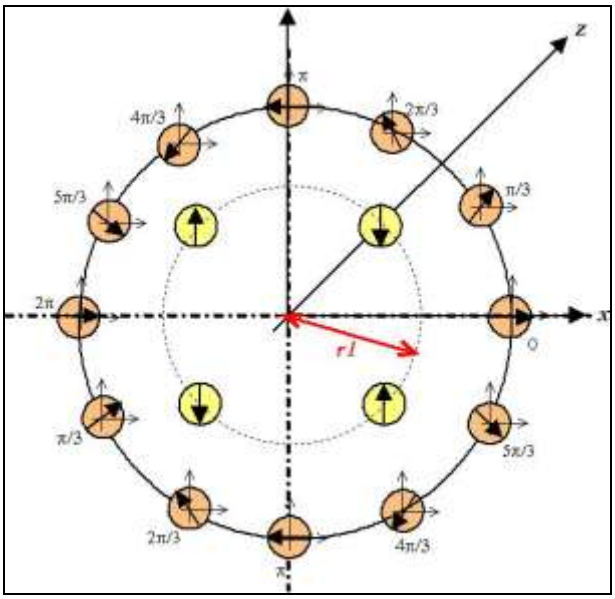

Figure 8: Direction of magnetization of the 8 shim magnets.

There are three variables that need to be optimized: *esp,* r1 and dH. The optimization objective is to determine the values for *esp*, r1 and dH that maximize the volume for an inhomogeneity of 100 ppm. The flow chart shown in Figure 9 describes the optimization process implemented with Mathematica software and the calculation of the magnetic field with Radia software. To avoid the superposition of the main magnets and the shim magnets, we set the range of r1 from 15 to 23 mm and the one for *esp* ranging from 0.1 to 0.6 mm. The optimal value for *esp,* considered here, is different from the value considered before because of the presence of shim magnets.

Each step of increase of r1 is 1 mm while correspondent value of esp is 0.1 mm. Each possible values of r1 is placed in a matrix. The corresponding magnetic field and then the three coordinates (x,y,z) for an homogeneity lower than 100 ppm are also determined. For each value of r1, we have a value for the homogeneous volume. The value of r1 leading to the highest value of the volume will be saved. The same process is repeated with the others parameters *esp* and dH. After a variation of one parameter, the variation is refined around the best value previously obtained. It's very important to choose good initial conditions and started the variation of one parameter with reliable value for the others parameters. This method was preferred to the use of Mathematica software optimization functions, as FindMaximum.

The magnetic field inhomogeneity calculated by Radia and by Ansys are in good agreement. However, Ansys gives always smaller useful volumes than those obtained by Radia due to the method of calculation. This can be explained by the fact that Radia result is the highest value at the region edge while Ansys compute the mean value for the overall region.

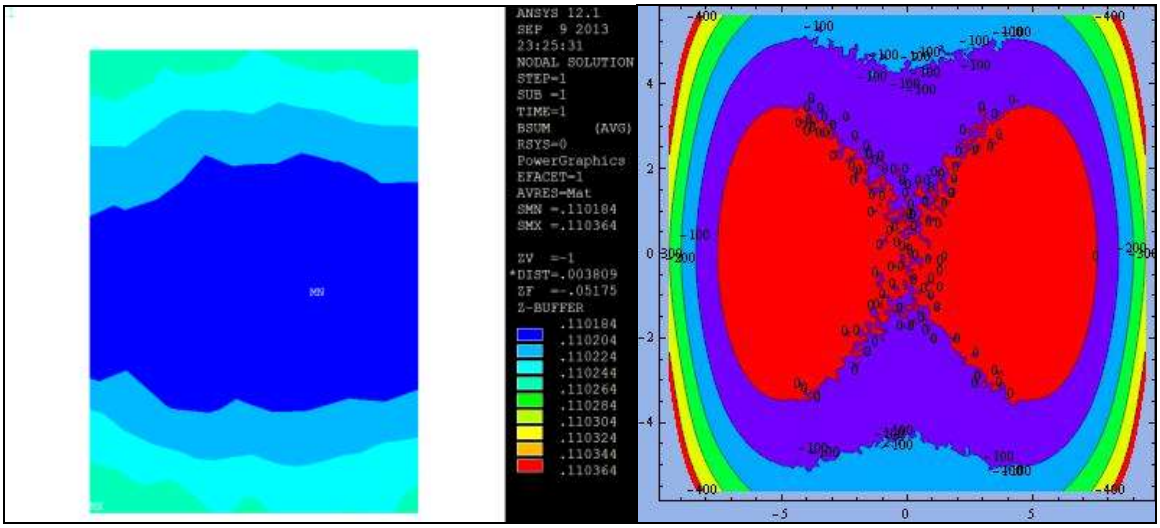

(a) Before shimming. (b) After shimming.

Figure 10: Magnetic field homogeneity in the xOy plane and z = 0.

The Figure 11 shows great improvement of homogeneity along Oz axis. The size of the homogeneous region increases drastically in length from 8 mm to 20 mm. This is confirmed by the stability of the magnetic field profile of the Figure 12.

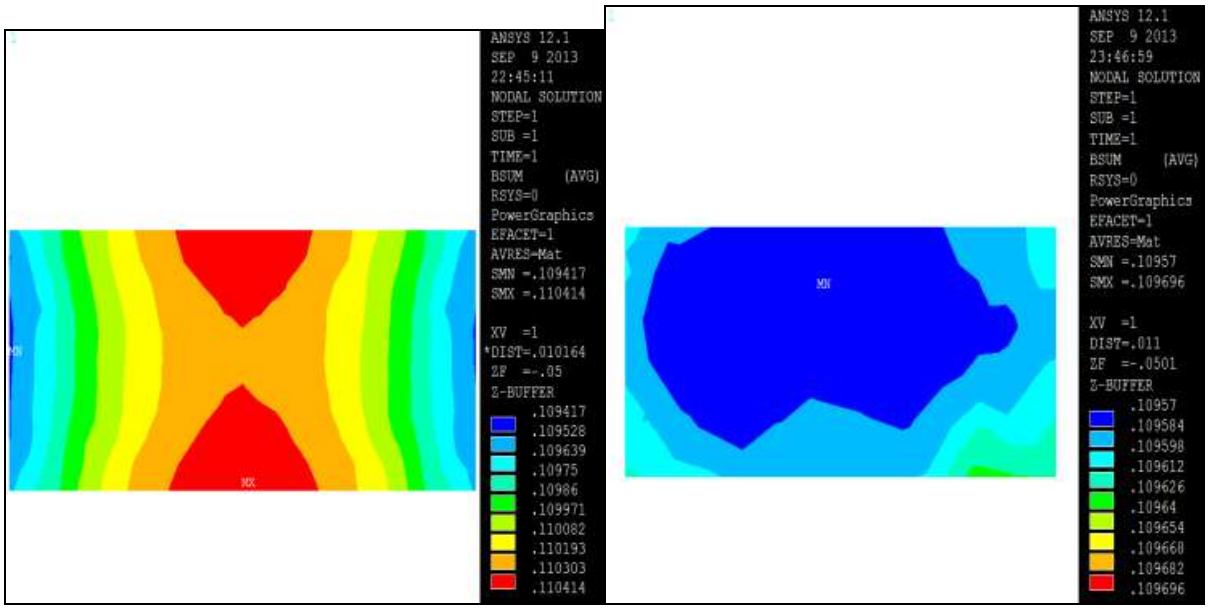

(a) Before shimming. (b) After shimming.

Figure 11: Magnetic field homogeneity in the region 8 x 20 mm^2 along Oz axis

(a) Shim magnets that can move along three degrees of freedom.

(b) Halbach prototype with the slide-blocks used to move the shim magnets in radial direction.

Figure 14: Picture of the prototype with shim magnets.

Each shim magnet shown on the Figure 14 is glued in a nonmagnetic cylinder. These cylinders can rotate, move along the longitudinal axis and slide along the radius of the prototype to find the optimal position of the shim magnets. These cylinders are placed in the holes of sliding-blocks moving on the four apertures of an aluminum frame concentric with the prototype.

b. Experimental setup

The magnetic field is measured by the digital gaussmeter Hirst GM08 with sensitivity limit of 10^{-4} T in the range 0 – 0.299 T. The micropositioner Signatone S-926 is used to control the probe movement in three directions as shown in the Figure 15. The resolution is 254 μm per knob revolution. Matlab software carries out the plotting of the measurable values.

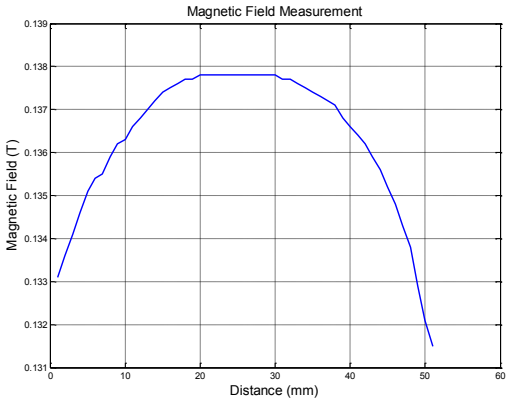

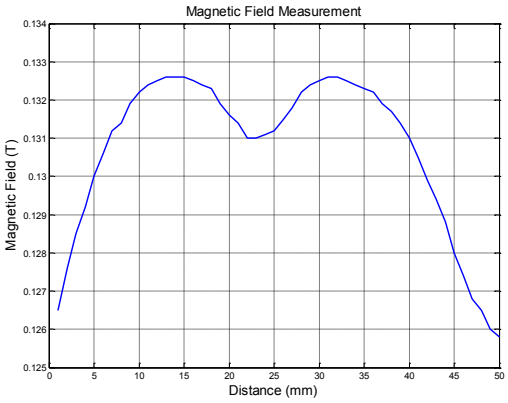

(c) *esp = 2.4 mm.* (d) *esp = 6.4 mm.*

Figure 16: Magnetic field profiles in Oz direction for different esp values.

The magnetic field distribution shown in Figure 17, is measured at z = 0, in the region 6 x 6.5 mm² (xOy). In this region, the homogeneity value is respectively 1399 ppm calculated by formula (1) and 380 ppm obtained by simulation. It means that the measurable homogeneity is approximately 3.5 times worse than that simulated (Figure 3-b).

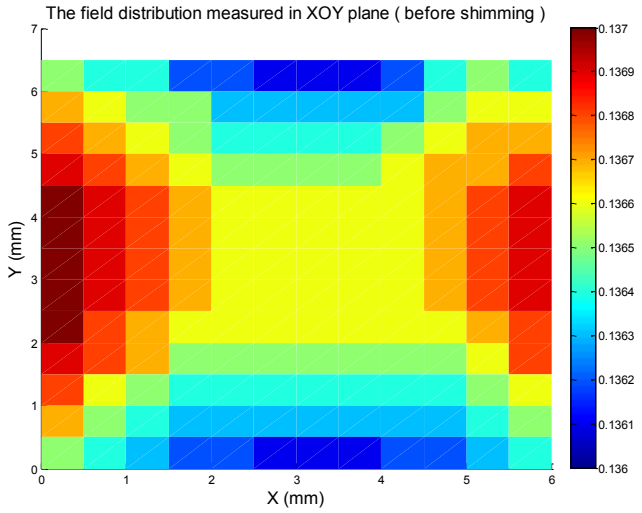

Figure 17: The magnetic field distribution in xOy plane obtained by measurement before shimming.

Figure 18 shows the magnetic field distribution measurement in xOz plane in the region of 7 x 20 mm². In this region the homogeneity calculated by formula (1) is equal to 1426 ppm. This homogeneity is of 4415 ppm in the volume of 6 x 7 x 20 mm^3.

The magnetic field distribution is similar to the simulation as shown in the Figure 4.

5.8 times worse than the simulated value. The measured and simulated field distribution in xOz plane are similar as shown in the Figure 4.

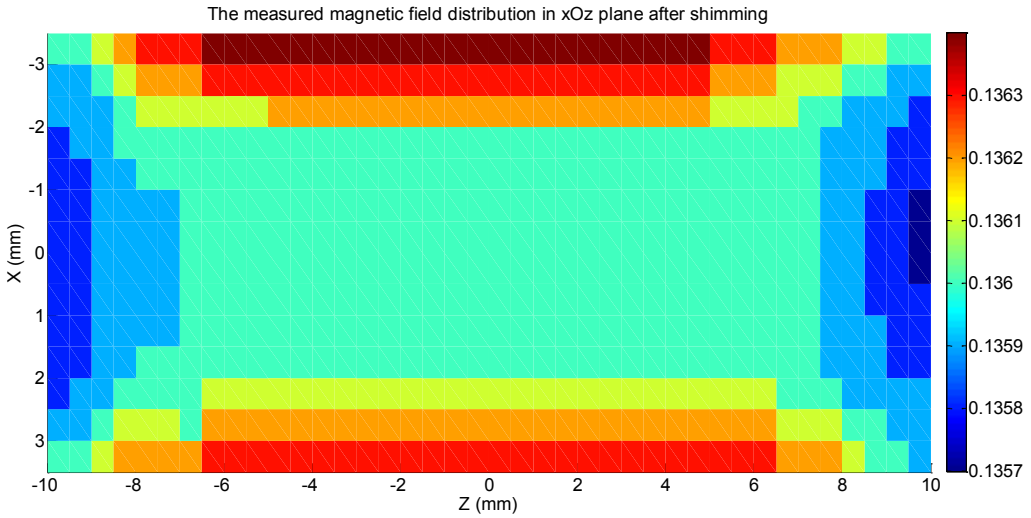

Figure 20: The magnetic field homogeneity in xOz plane after shimming.

VI. DISCUSSION

The difference between the simulated and measured values of the magnetic field homogeneity is due to the poor quality of the magnets. There is a large dispersion of the magnets properties. For our prototype we selected 24 magnets among 27 having a similar magnetic field strength and the magnets 5, 22 and 23 was rejected. This was done with the measurement of the magnetic field on each tip of the magnet cylinder. Table 3 shows the value of B_1 and B_2 for 27 magnets and the misalignment angle α. B_1 and B_2 are respectively the magnetic field in the vicinity of the two faces of the magnet cylinder as shown on the

Figure 21. The average value of the magnetic field is around 27.3 mT. The misalignment angle represents the error of orientation of the radial direction of the magnetic field on each face. In ideal case, this angle value is zero but for some magnets this value can reach 17 degrees and the consequence, is an error of homogeneity of the magnetic field.

Table 3: Magnetic field and misalignment angle measured on each tip of the 27 magnets.

Magnet	**1**	**2**	**3**	**4**	**5**	**6**	**7**	**8**	**9**	**10**
B_1 (mT)	27.3	27.2	27.3	27.2	27.3	27.2	27.1	27.0	26.9	27.0
B_2 (mT)	27.2	27.1	27.5	27.1	27.0	27.1	27.2	26.9	27.0	27.2
α (degree)	0	0	8	9	17	8	0	0	0	12
Magnet	**11**	**12**	**13**	**14**	**15**	**16**	**17**	**18**	**19**	**20**
B_1 (mT)	27.4	27.2	27.2	27.2	27.3	27.3	27.3	27.4	27.4	27.4
B_2 (mT)	27.5	27.0	27.2	27.4	27.4	27.3	27.5	27.4	27.5	27.2
α (degree)	0	10	0	12	0	0	12	0	0	8
Magnet	**21**	**22**	**23**	**24**	**25**	**26**	**27**			
B_1 (mT)	27.3	27.2	27.6	27.3	27.4	27.4	27.3			
B_2 (mT)	27.3	27.5	27.5	27.4	27.3	27.5	27.4			
α (degree)	0	16	4	6	9	7	8			

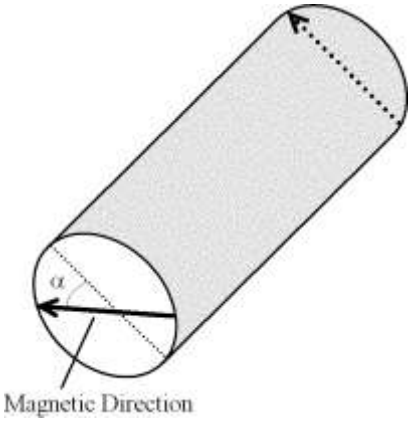

(a) Magnet cylinder with B_1 and B_2 the magnetic field in the vicinity of its two faces and the misalignment angle α.

(b) Picture of Magnet cylinder.

Figure 21: A prototype of Magnet cylinder.

In the following, we will study the impact of the error of the misalignment of magnetic directions and the reducing of the homogeneity. During the simulation, an angle error of 3 degrees of the magnetic field direction for four magnets is considered as shown in the Figure 22.

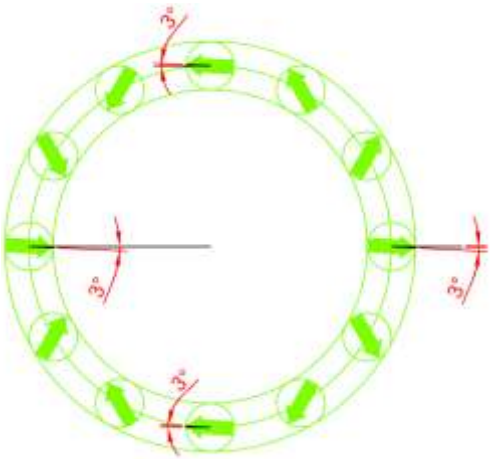

Figure 22: Misalignment of the magnetic direction for four magnets.

The results of simulation show that the inhomogeneity of magnetic field drastically increases to 2750 ppm in the region of 6 x 6.5 mm^2 (xOz plane) in comparison to 380 ppm, the value without misalignment error. As shown in the Figure 23, the magnetic field distribution is similar to the measurement.

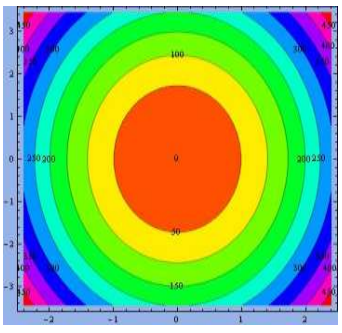

(a) Simulation without misalignment error of the direction of the magnetic field.

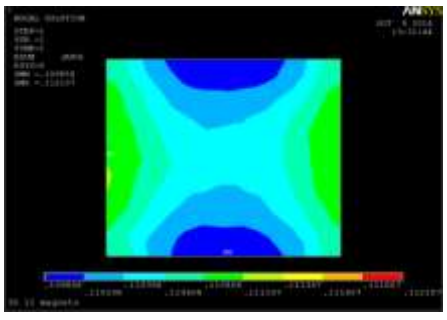

(b) Simulation with 3 degree misalignment error.

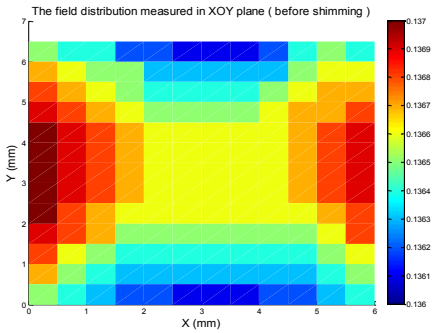

(c) Field distribution measurement of the prototype.

Figure 23: The magnetic field distribution in xOz plane, for ideal case and with error of misalignment of the direction of the magnetic field.

VII. CONCLUSION

The study presented here depicts two methods of simulation and the main measurement results of a light weight NMR portable Halbach type magnet. We described the optimization process of this permanent magnet designed with two rings of 12 magnets each one, that provide a magnetic field B0 around 0.1 T. The simulation results have been published in [22]. The study describes the used based on the Radia software process, for calculate and simulate the magnetic field B0 and its homogeneity. We verified also those results with the finite element software Ansys multiphysics. The obtained results with the two softwares are in good agreement. Based on the software analysis, we simulated the homogeneity of magnetic field and optimized the gap *esp* of the two consecutive rings to increase the size of the homogeneous region. The optimum gap length is around *esp*= 0.8 mm. The measurement of the magnetic field profile for different values of the gap *esp* between the two rings give a similar value of the optimal gap.

To compensate for the magnetic field inhomogeneity caused by the errors of fabrication process and the dispersion of the magnetic properties of the magnets, we used eight small shim magnets placed at the center of the device. By optimizing their position, the homogeneity had been significantly improved. The results of optimization shows that the homogeneity for a given volume (7 x 8 x 20 mm^3) is improved 18 times in comparison to the same configuration without shim magnets. Thus the value of the homogeneity decrease from 4320 ppm to 230 ppm.

For a given volume of 6 x 7 x 20 mm^3, the measurement of the magnetic field variation, shows the same homogeneity improvement, using the shim magnets. Thus the homogeneity is of 1335 ppm while it was of 4415 ppm for the case without shim magnets. The magnetic field homogeneity was enhanced of a 3.3 factor. However, there is still a difference between the simulation and the measurement, which could be explained by the poor quality of the magnets. For each used magnets for the NMR device design, the magnetic field on the tip of the cylindrical magnet and the misalignment angle of the radial magnetic field were

measured. The misalignment angle could be as high as 17 degrees. The simulations with some misalignment angle error of 3 degree on four magnets were performed and the same shape of the magnetic field distribution was obtained. Thus we attribute the difference between the simulation and the measurement to the misalignment angle of the magnets.

Despite these results, there's a good agreement between the simulation results and the measurement.

REFERENCES

[1] S. Anferova, V. Anferov, M. Adams, P. Blümler, N. Routley, K. Hailu, K. Kupferschläger, M. j. d. Mallett, G. Schroeder, S. Sharma, and B. Blümich, "Construction of a NMR-MOUSE with short dead time," *Concepts Magn. Reson.*, vol. 15, no. 1, pp. 15–25, Mar. 2002.

[2] G. Moresi and R. Magin, "Miniature permanent magnet for table-top NMR," *Concepts Magn. Reson.*, vol. 19B, no. 1, pp. 35–43, 2003.

[3] G. Navon, U. Eliav, D. E. Demco, and B. Blümich, "Study of order and dynamic processes in tendon by NMR and MRI," *J. Magn. Reson. Imaging*, vol. 25, no. 2, pp. 362–380, Feb. 2007.

[4] F. J. Rühli, T. Böni, J. Perlo, F. Casanova, M. Baias, E. Egarter, and B. Blümich, "Non-invasive spatial tissue discrimination in ancient mummies and bones in situ by portable nuclear magnetic resonance," *J. Cult. Herit.*, vol. 8, no. 3, pp. 257–263, Jul. 2007.

[5] B. Blümich, F. Casanova, J. Perlo, S. Anferova, V. Anferov, K. Kremer, N. Goga, K. Kupferschläger, and M. Adams, "Advances of unilateral mobile NMR in nondestructive materials testing," *Magn. Reson. Imaging*, vol. 23, no. 2, pp. 197–201, Feb. 2005.

[6] T. Poli, L. Toniolo, M. Valentini, G. Bizzaro, R. Melzi, F. Tedoldi, and G. Cannazza, "A portable NMR device for the evaluation of water presence in building materials," *J. Cult. Herit.*, vol. 8, no. 2, pp. 134–140, Apr. 2007.

[7] H. Pedersen, S. Ablett, D. Martin, M. J. Mallett, and S. Engelsen, "Application of the NMR-MOUSE to food emulsions," *J. Magn. Reson.*, vol. 165, no. 1, pp. 49–58, Nov. 2003.

[8] B. Blümich, V. Anferov, S. Anferova, M. Klein, R. Fechete, M. Adams, and F. Casanova, "Simple NMR-mouse with a bar magnet," *Concepts Magn. Reson.*, vol. 15, no. 4, pp. 255–261, Dec. 2002.

[9] W.-H. Chang, J.-H. Chen, and L.-P. Hwang, "Single-sided mobile NMR with a Halbach magnet," *Magn. Reson. Imaging*, vol. 24, no. 8, pp. 1095–1102, Oct. 2006.

[10] C. W. Windt, H. Soltner, D. van Dusschoten, and P. Blümler, "A portable Halbach magnet that can be opened and closed without force: The NMR-CUFF," *J. Magn. Reson.*, vol. 208, no. 1, pp. 27–33, Jan. 2011.

[11] X. Zhang, V. Mahesh, D. Ng, R. Hubbard, A. Ailiani, B. O'Hare, A. Benesi, and A. Webb, "Design, construction and NMR testing of a 1 tesla Halbach Permanent Magnet for Magnetic Resonance," in *COMSOL Users Conference, Boston*, 2005.

[12] K. Halbach, "Design of permanent multipole magnets with oriented rare earth cobalt material," *Nucl. Instrum. Methods*, vol. 169, no. 1, pp. 1–10, Feb. 1980.

[13] H. Raich and P. Blümler, "Design and construction of a dipolar Halbach array with a homogeneous field from identical bar magnets: NMR Mandhalas," *Concepts Magn. Reson. Part B Magn. Reson. Eng.*, vol. 23B, no. 1, pp. 16–25, Oct. 2004.

[14] H. Soltner and P. Blümler, "Dipolar Halbach magnet stacks made from identically shaped permanent magnets for magnetic resonance," *Concepts Magn. Reson. Part A*, vol. 36A, no. 4, pp. 211–222, Jul. 2010.

[15] B. P. Hills, K. M. Wright, and D. G. Gillies, "A low-field, low-cost Halbach magnet array for open-access NMR," *J. Magn. Reson.*, vol. 175, no. 2, pp. 336–339, Aug. 2005.

[16] E. Danieli, J. Mauler, J. Perlo, B. Blümich, and F. Casanova, "Mobile sensor for high resolution NMR spectroscopy and imaging," *J. Magn. Reson.*, vol. 198, no. 1, pp. 80–87, May 2009.

[17] C. Hugon, F. D'Amico, G. Aubert, and D. Sakellariou, "Design of arbitrarily homogeneous permanent magnet systems for NMR and MRI: Theory and experimental developments of a simple portable magnet," *J. Magn. Reson.*, vol. 205, no. 1, pp. 75–85, Jul. 2010.

[18] R. C. Jachmann, D. R. Trease, L.-S. Bouchard, D. Sakellariou, R. W. Martin, R. D. Schlueter, T. F. Budinger, and A. Pines, "Multipole shimming of permanent magnets using harmonic corrector rings," *Rev. Sci. Instrum.*, vol. 78, no. 3, p. 035115, Mar. 2007.

[19] "Radia Introduction." [Online].
http://www.esrf.eu/Accelerators/Groups/InsertionDevices/Software/Radia/Documentation/Introduction. [Accessed: 05-Oct-2014].

[20] "ANSYS - Simulation Driven Product Development." [Online]. Available:
http://www.ansys.com/. [Accessed: 13-Aug-2014].

[21] “HKCM MAGNETS from STOCK, from FACTORY & MAGNETS ON DEMAND.” [Online]. Available: https://www.hkcm.de/expert.php. [Accessed: 11-Jul-2014].

[22] P. Poulichet, Hung Dang Phuc, Tien Truong Cong, Latifa Fakri-Bouchet, Abdennasser Fakri, and Christophe Delabie, “Simulation and optimisation of homogeneous permanent magnet for portable NMR applications,” *8th International Conference on Sensing Technology*, Liverpool, UK., 04-Sep-2014.